Electronic Supplementary information

Aggregation-Induced Emission Enhancement and Aggregation-Induced Circular Dichroism of Chiral Pentaphenylpyrrole Derivatives and Their Helical Self-Assembly

Longlong Zhang,[a] Kaichang Liang,[a] Lichao Dong,[b] Peipei Yang,[a] Yuanyuan Li,[a] Xiao Feng,[a] Junge Zhi,*[a] Jianbing Shi,[b] Bin Tong[b] and Yuping Dong*[b]

[a] School of Chemistry and Chemical Engineering, Beijing Key Laboratory of Photoelectronic/Electrophotonic Conversion Materials, Beijing Institute of Technology, Beijing 100081, China. E-mail: zhijunge@bit.edu.cn

[b] School of Materials Science and Engineering, Beijing Institute of Technology, Beijing 100081, China. E-mail: chdongyp@bit.edu.cn

1. ^{1}H NMR, MS and IR spectra and TGA curves of the target compounds

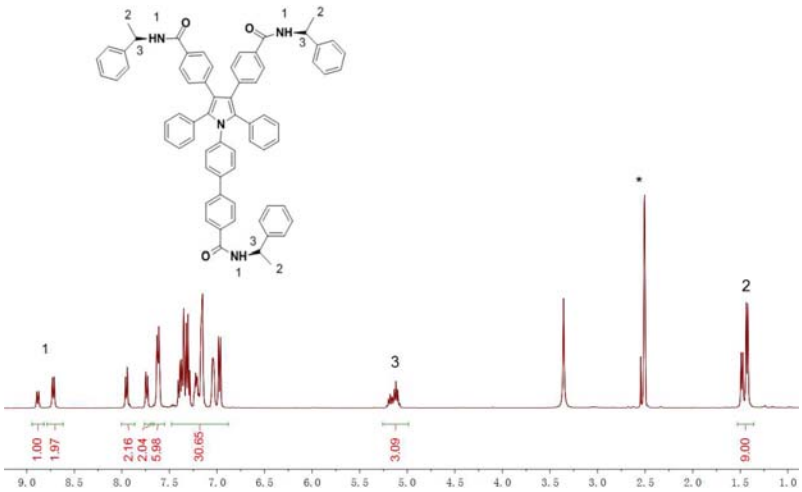

(a) (*S*)-PPPtriAm

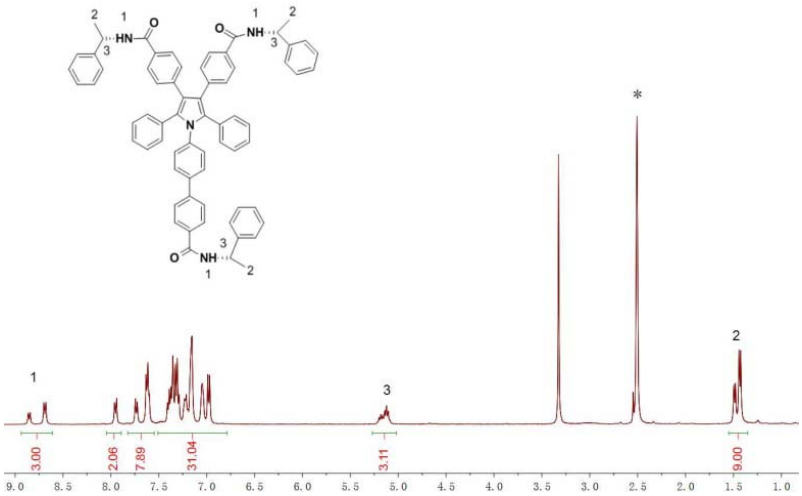

(b) (*R*)-PPPtriAm

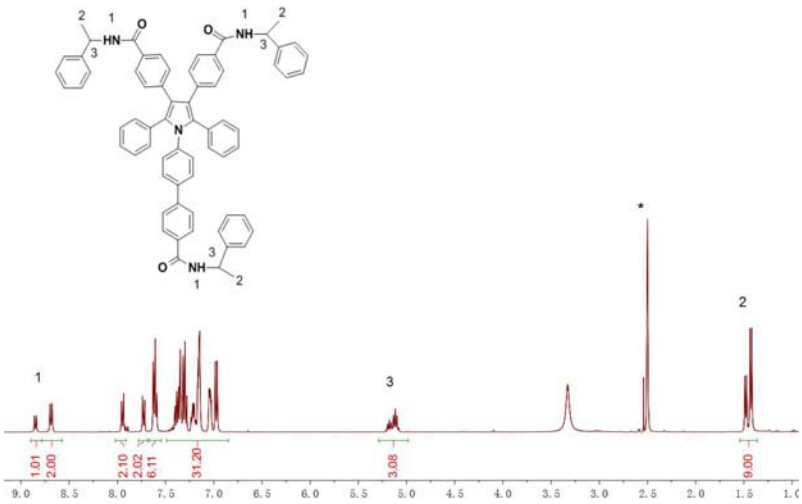

(c) *rac*-PPPtriAm

Fig. S1. ^{1}H NMR spectra of (*S*)-PPPtriAm, (*R*)-PPPtriAm and *rac*-PPPtriAm

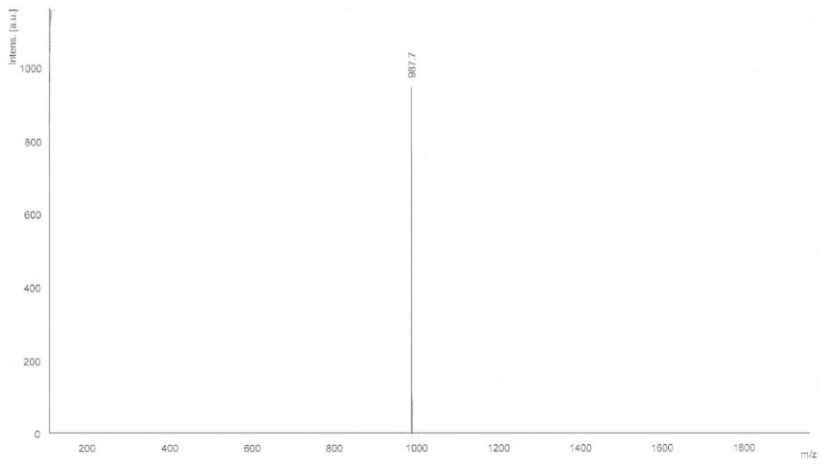

(a) (*S*)-PPPtriAm

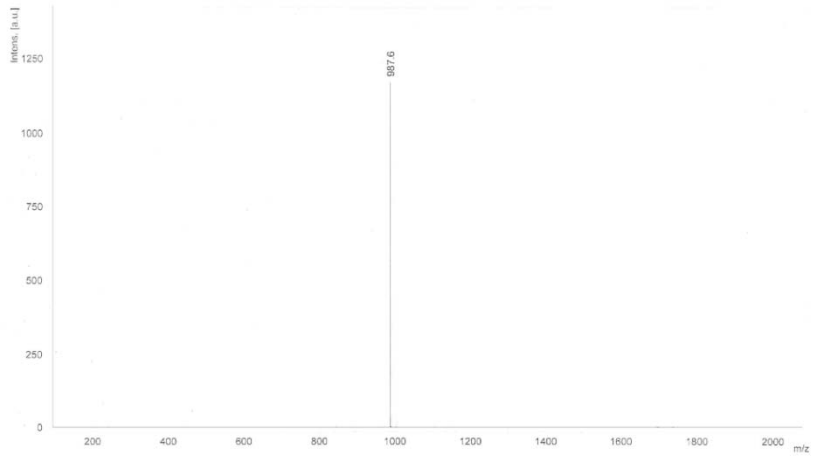

(b) (*R*)-PPPtriAm

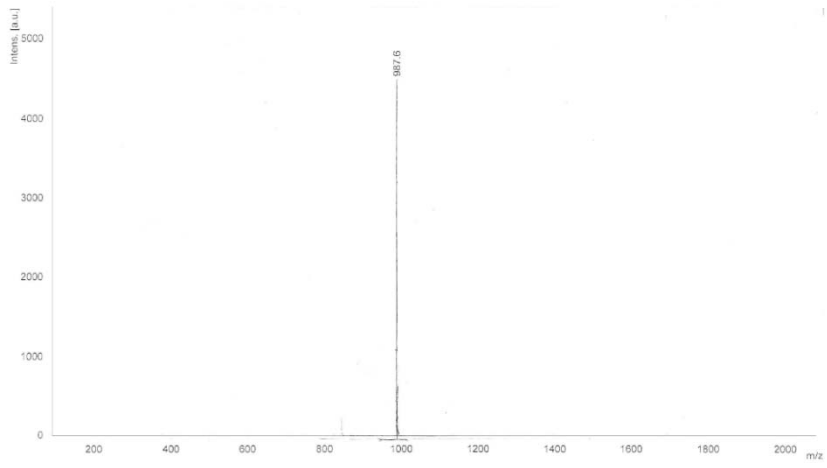

(c) *rac*-PPPtriAm

Fig. S2. Mass spectra of (*S*)-PPPtriAm, (*R*)-PPPtriAm and *rac*-PPPtriAm

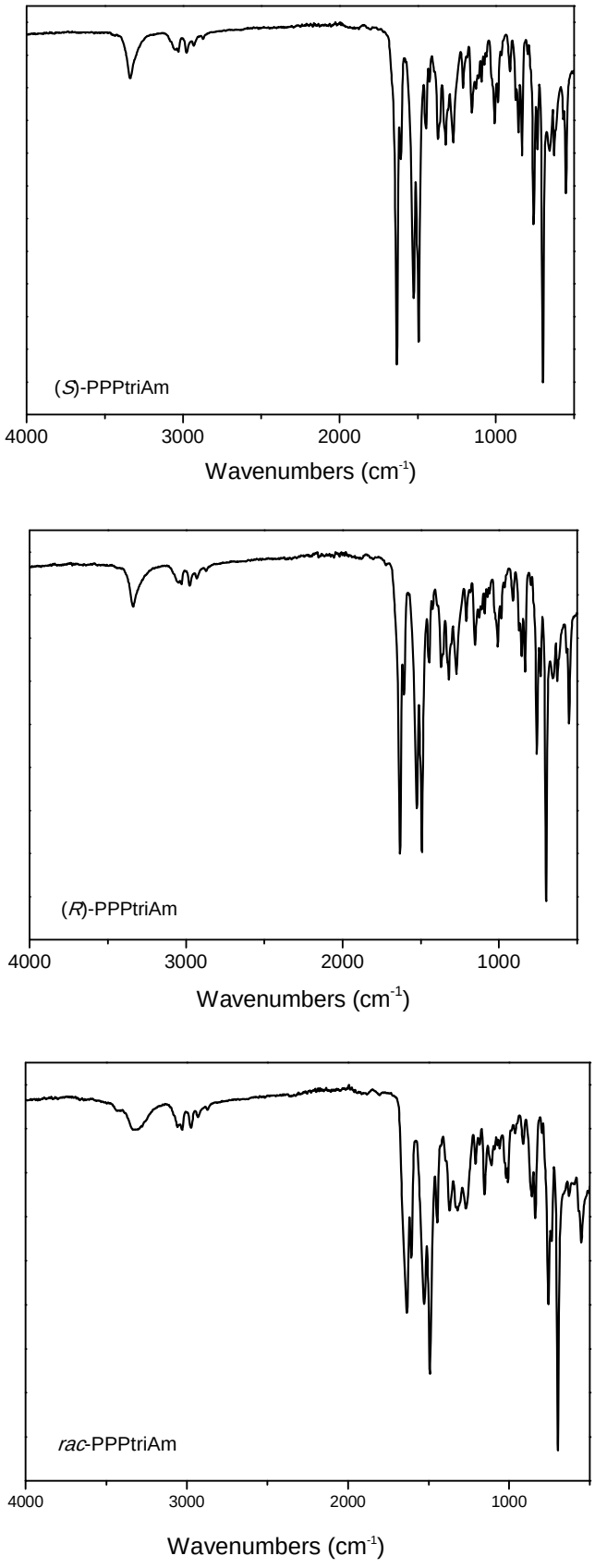

Fig. S3. IR spectra of (*S*)-PPPtriAm, (*R*)-PPPtriAm and *rac*-PPPtriAm

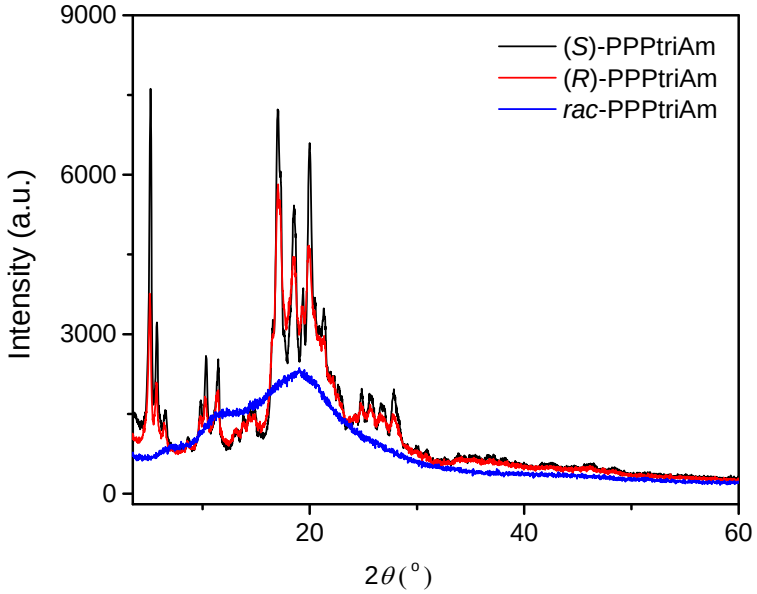

Fig. S4. XRD patterns of (*S*)-PPPtriAm, (*R*)-PPPtriAm and *rac*-PPPtriAm

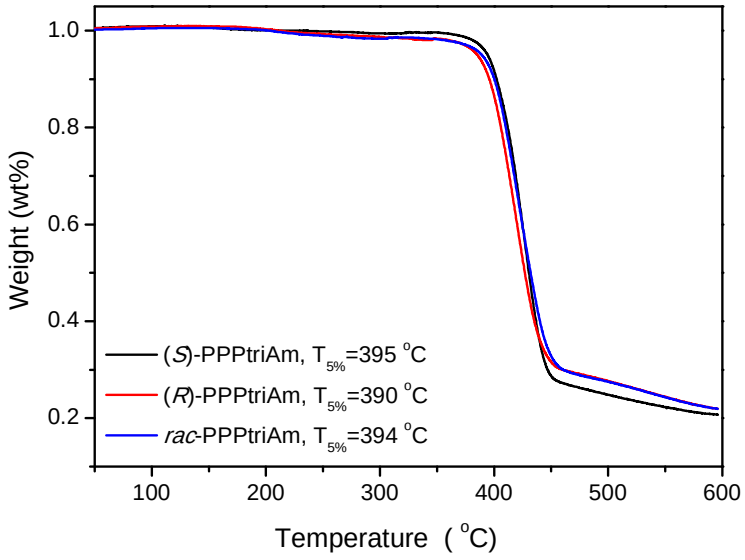

Fig. S5. TGA curves of (*S*)-PPPtriAm, (*R*)-PPPtriAm and *rac*-PPPtriAm

2. PL, UV-vis absorption and transmittance spectra of the target compounds

Table S1 The absolute quantum yields of target compounds in DMSO-H_2O mixtures

f_w (vol%)	Φ_F		
	(*R*)-PPPtriAm	(*S*)- PPPtriAm	*rac*- PPPtriAm
0	5.28	5.47	6.44
30	3.01	3.66	3.69
40	14.53	15.48	14.10
50	12.09	12.42	12.21
60	10.18	13.76	12.42
70	9.18	9.42	9.15
80	6.06	9.89	9.26

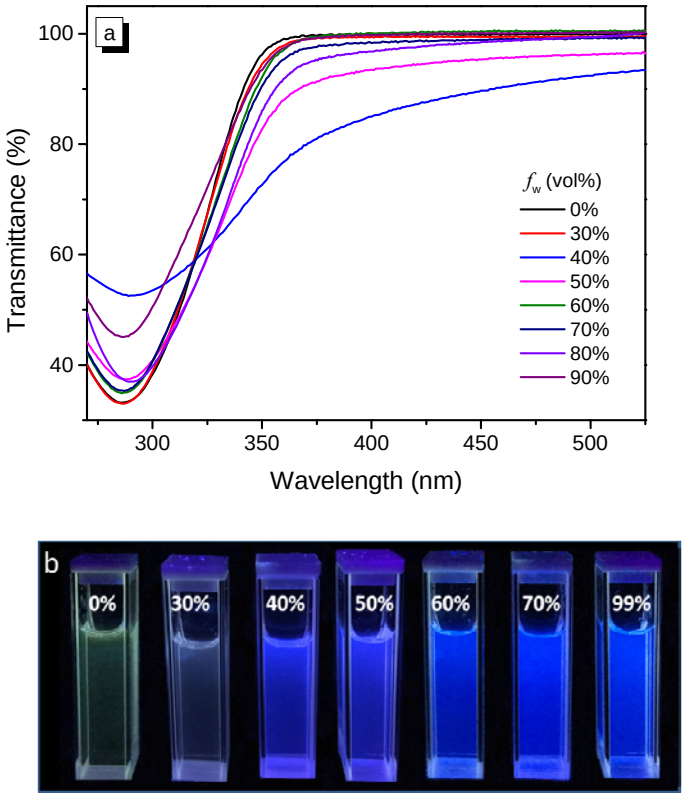

Fig. S6. UV-vis transmittance (a), photographs taken under 365 nm UV light (b) of (*S*)-PPPtriAm in DMSO-water mixtures with different water fraction (f_w) (Concentration: 10 μM)

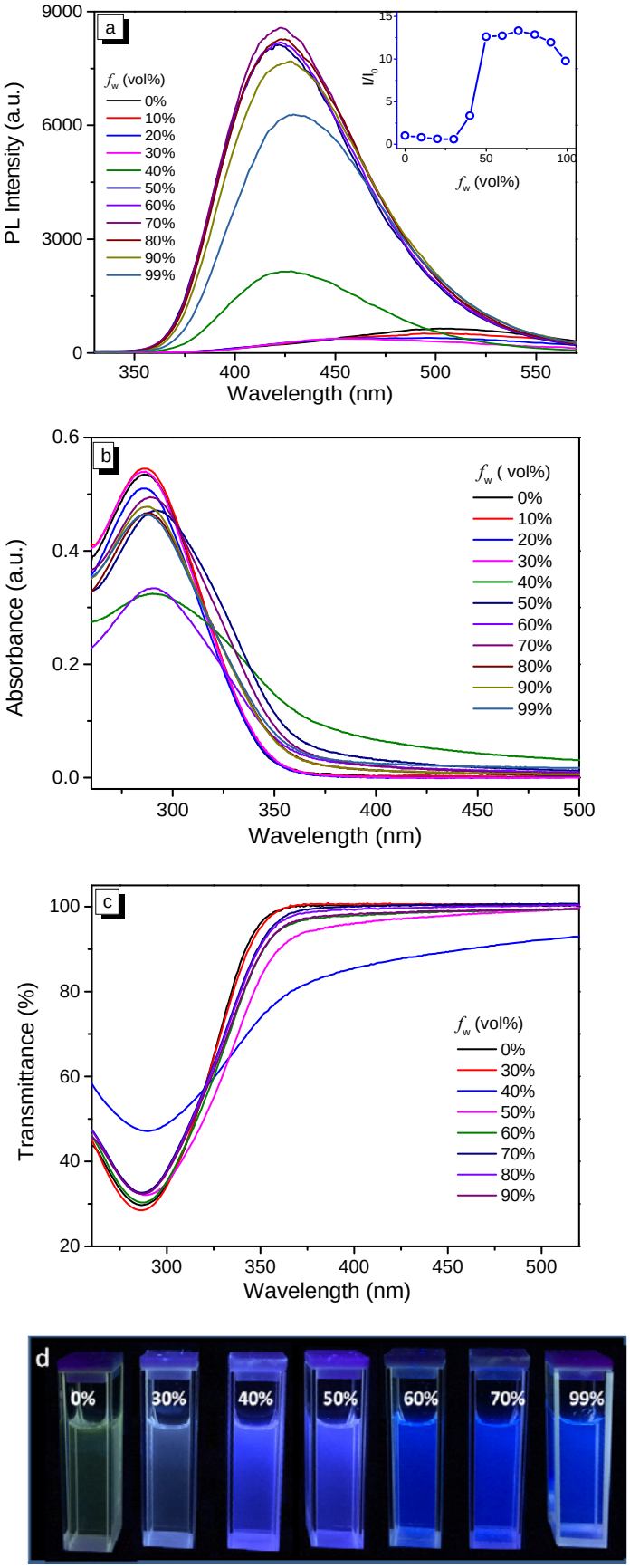

Fig. S7. PL spectra (a), UV-vis absorption spectra (b), Transmittance (c), photographs taken under 365 nm UV light (d) of (*R*)-PPPtriAm in DMSO-water mixtures with different f_w (Inset: Plot of I/I$_0$ versus f_w in DMSO-water mixtures), (λ_{ex} = 290 nm, Concentration: 10 μM)

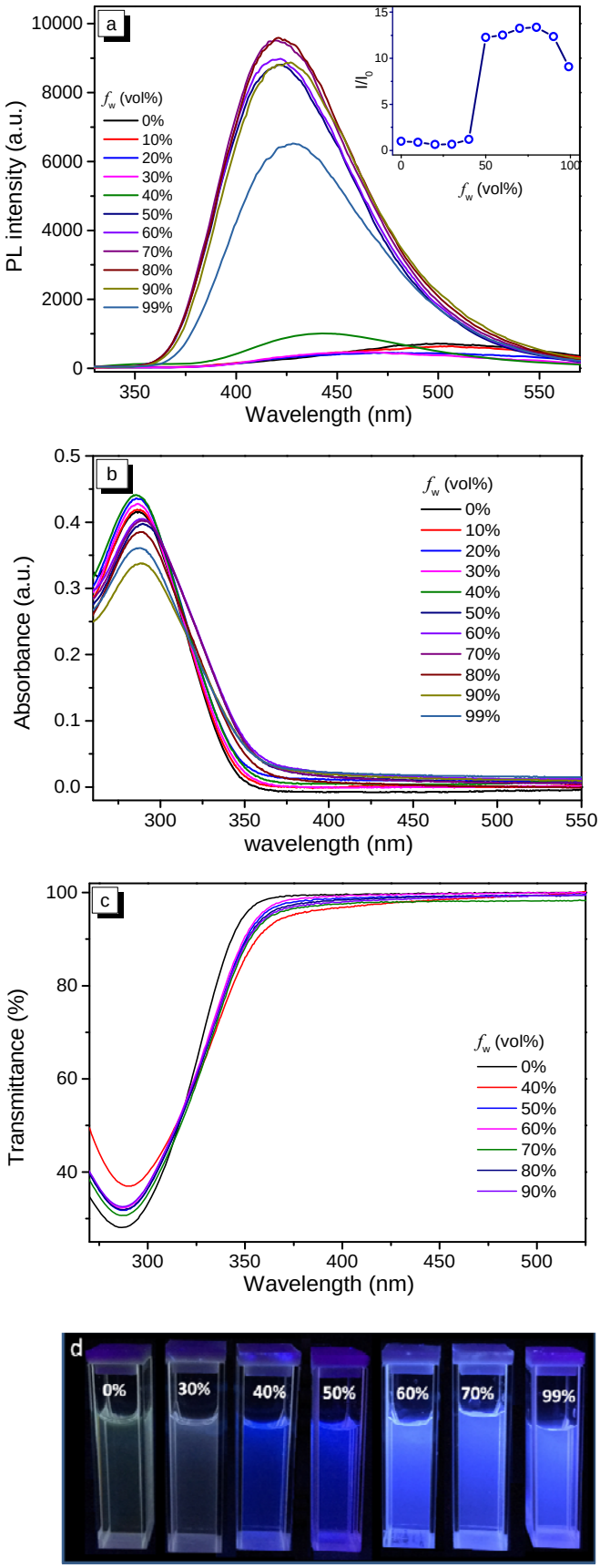

Fig. S8. PL spectra (a), UV-vis absorption spectra (b), Transmittance (c), Photographs taken under 365 nm UV light (d) of *rac*-PPPtriAm in DMSO-water mixtures with different f_w (Inset: Plot of I/I_0 versus f_w in DMSO-water mixtures), (λ_{ex} = 290 nm, Concentration: 10 μM)

3. Particle size distributions of the target compounds

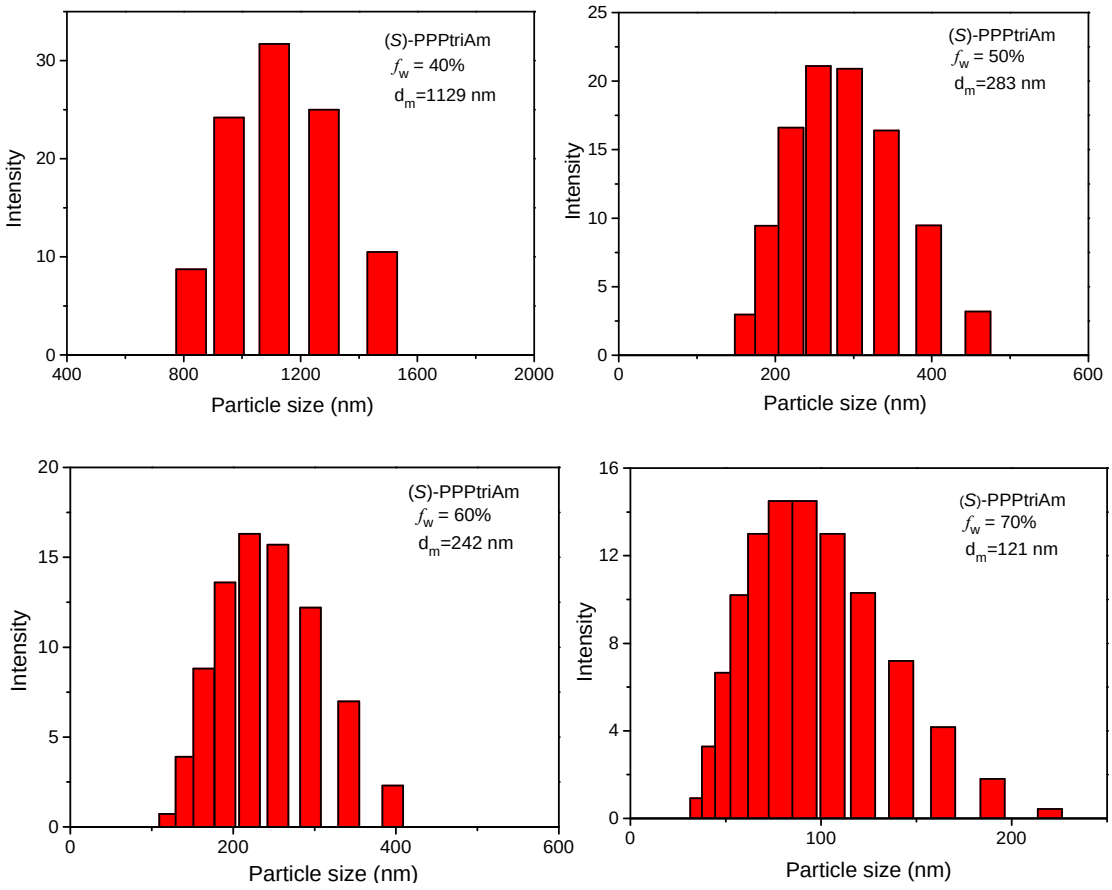

(a) (*S*)-PPPtriAm

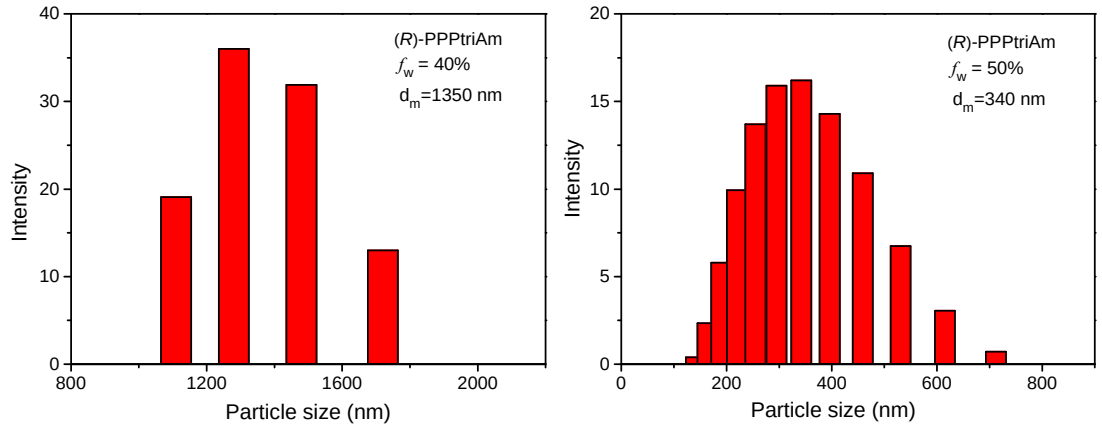

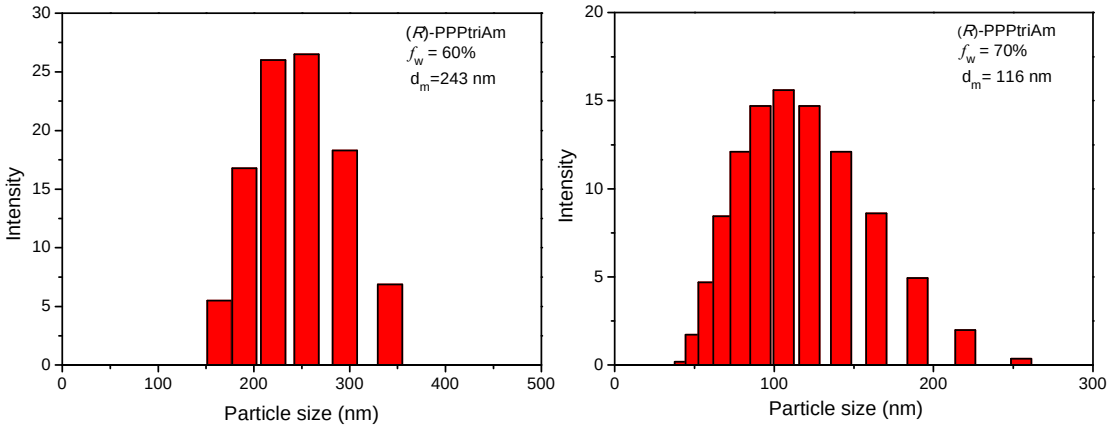

(b) (*R*)-PPPtriAm

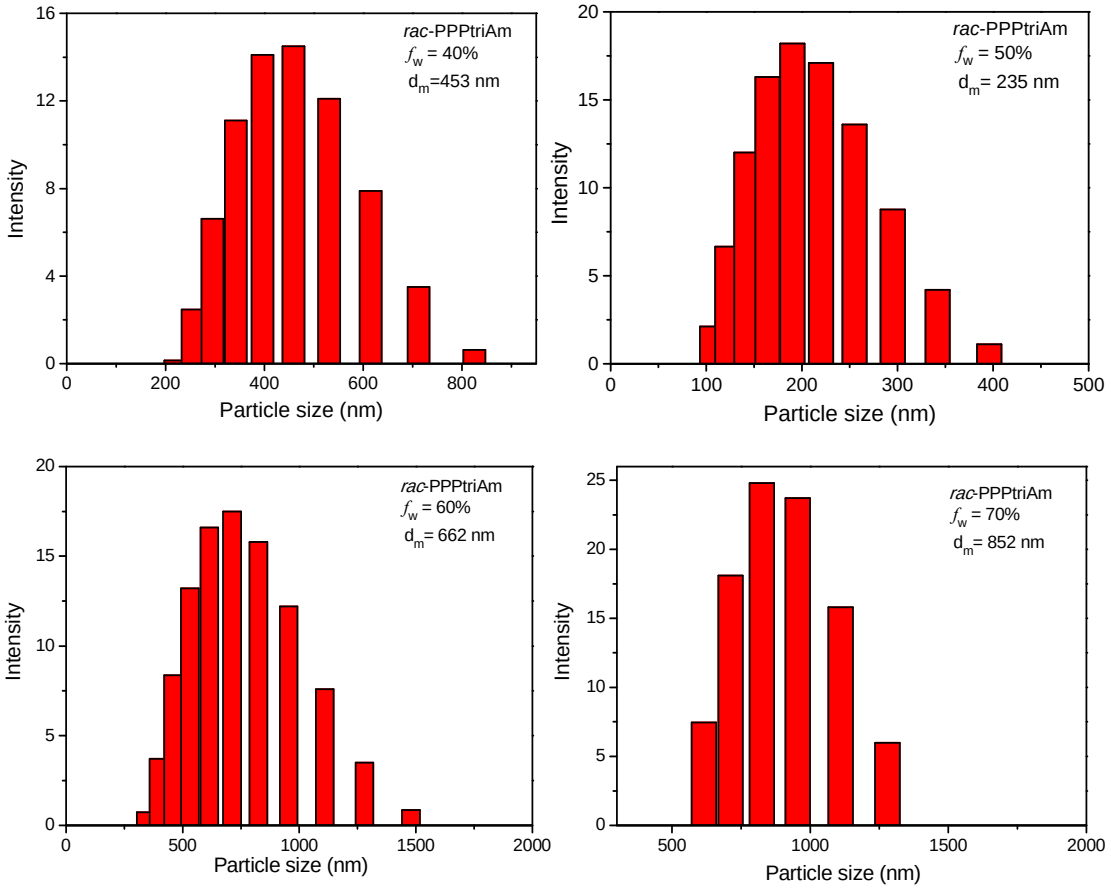

(c) *rac*-PPPtriAm

Fig. S9. Particle size distributions of (*S*)-PPPtriAm (a), (*R*)-PPPtriAm (b) and *rac*-PPPtriAm (c) in DMSO-water mixtures with different f_w (d_m is the mean diameter; Concentration:10 μM)

4. Molecular orbital amplitude of the target compounds

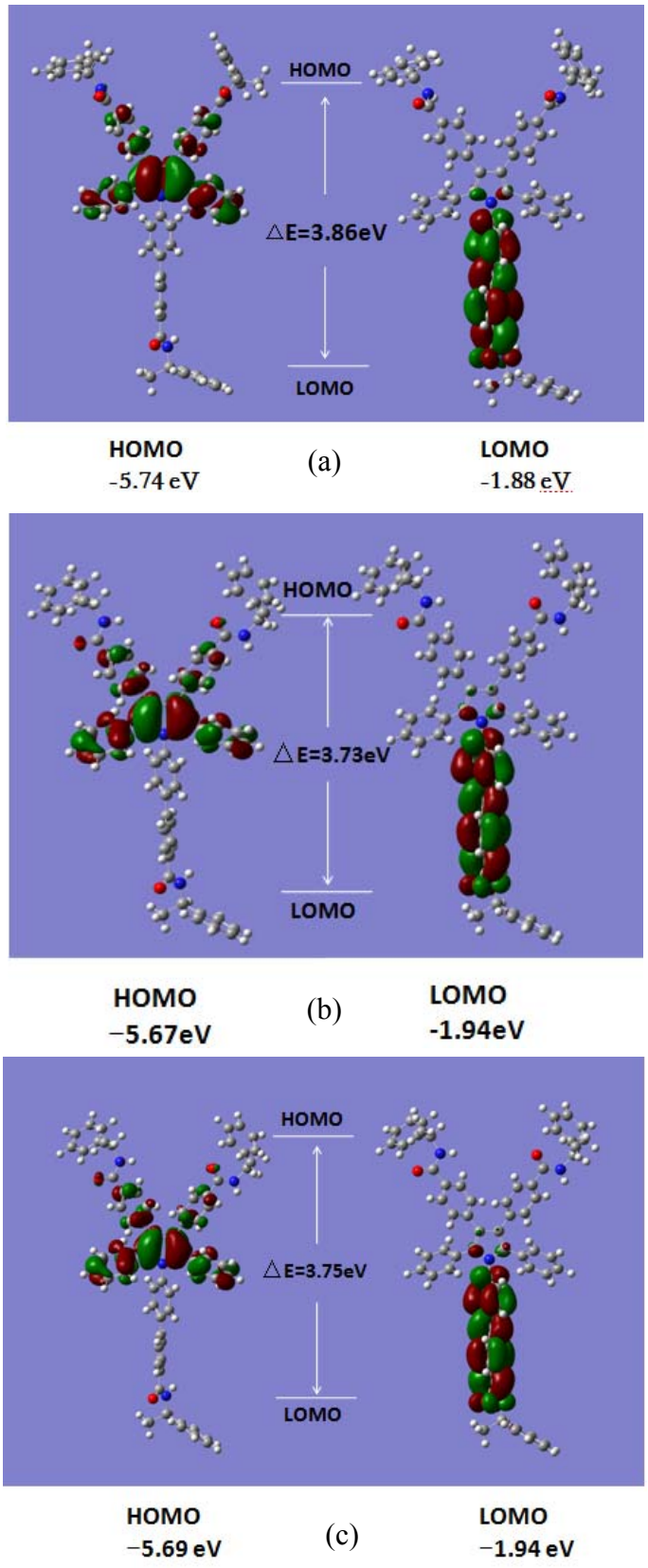

Fig. S10. Molecular orbital amplitude plots of HOMO and LUMO energy levels of compounds (*S*)-PPPtriAm (a), (*R*)-PPPtriAm (b) and *rac*-PPPtriAm (c)

5. CD spectra and dissymmetry factor of the target compounds

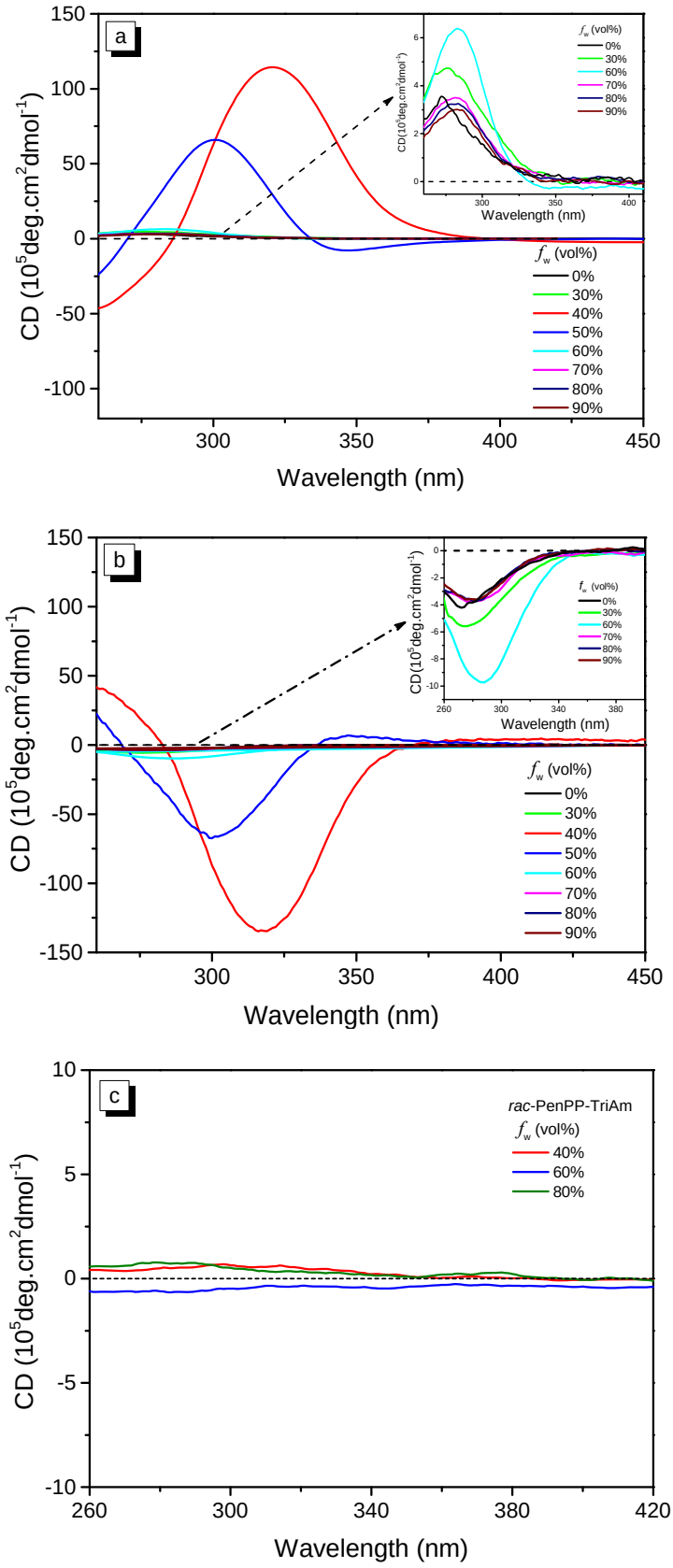

Fig. S11. CD spectra of compounds (*S*)-PPPtriAm (a), (*R*)-PPPtriAm (b), *rac*-PPPtriAm (c) in DMSO-water mixtures with different f_w (Concentration: 10 μM)

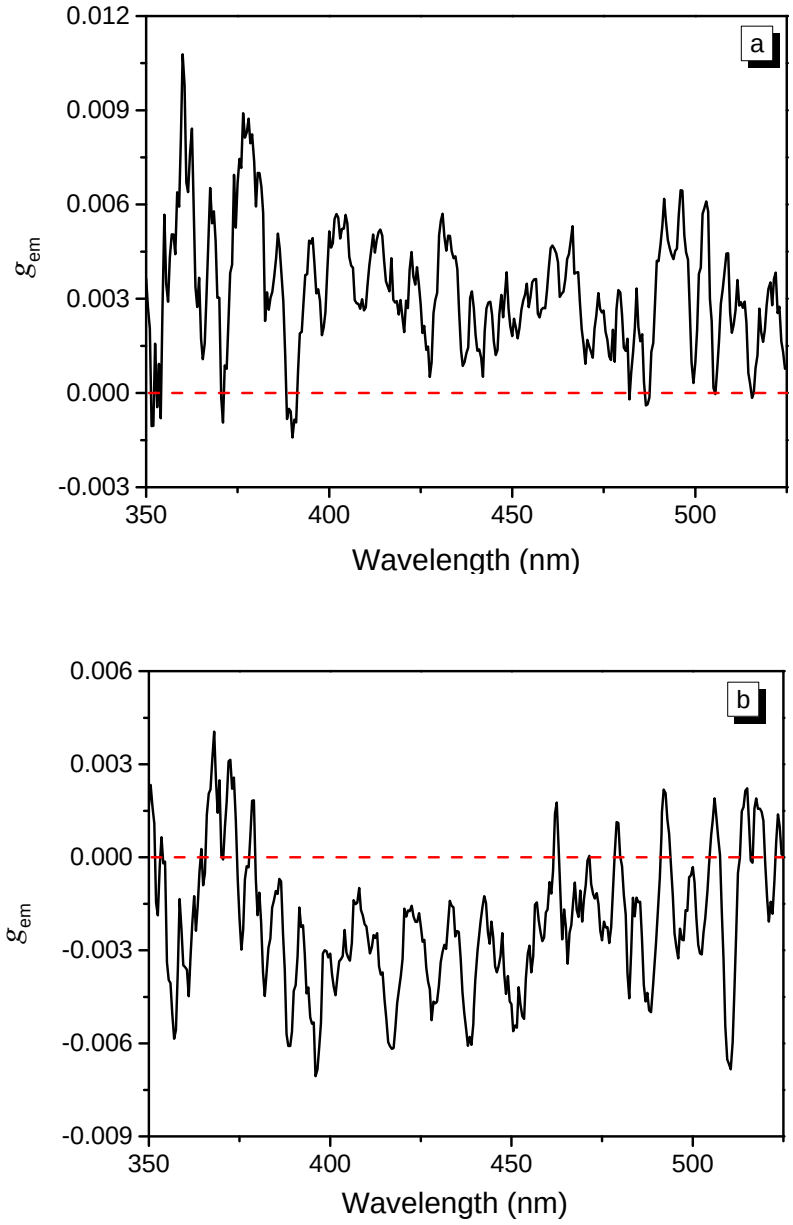

Fig. S12. Dissymmetry factor (g_{em}) of chiral compounds (*S*)-PPPtriAm (a) and (*R*)-PPPtriAm (b) in DMSO-water mixtures at f_w of 40%, (λ_{ex} = 290 nm, Concentration: 10 μM).